13th International Conference on
Structural Health Monitoring of Intelligent Infrastructure
DOI: 10.3217/978-3-99161-057-1-099

Concrete signature in long-term Distributed Fiber Optic Strain Sensing: Challenges and opportunities for Structural Health Monitoring

Lisa Ulbrich[1], ORCID, Alessia Abbozzo[2], ORCID, Frank Jesse[1], ORCID, Marco di Prisco[2], ORCID
[1]Hentschke Bau GmbH, Department of Research and Development, Zeppelinstr. 15, 02625 Bautzen, Germany
[2]Department of Civil and Environmental engineering, Politecnico di Milano, P.za L. da Vinci, 32 – 20133 Milano, Italy.
email: Ulbrich.Lisa@hentschke-bau.de, Jesse.Frank@hentschke-bau.de, alessia.abbozzo@polimi.it, marco.diprisco@polimi.it

ABSTRACT: In recent years, Distributed Strain Sensing (DSS), utilizing optical frequency domain reflectometry of Rayleigh backscatter, has gained significant prominence in the realm of Bridge Structural Health Monitoring (BSHM). Its key advantage is its ability to provide continuous strain monitoring with high spatial resolution (0.65 mm) and an accuracy of up to 1 µm/m. This capability facilitates the monitoring of deformations and defects, as well as precise crack detection, the assessment of crack width and others.

However, publications on DSS based on Rayleigh backscattering often report local effects that are not linked to disturbances caused by the measurement principle, such as noise or anomalies in strain readings. These effects can complicate the evaluation of DSS data, particularly concerning crack detection and width measurement, as well as tasks like detecting tension wire breakages. There have been theories, suggesting that these local effects may stem from micro-cracks or inhomogeneities within the concrete matrix, yet further investigations into this phenomenon are lacking.

Within this paper the phenomenon of local effects, henceforth referred to as the *concrete signature*, has been investigated on multiple time scales during. The analysis utilizes data from the openLAB research bridge in Bautzen, Germany. Possible reasons for the development and behavior of *concrete signature* are discussed, along with the challenges and opportunities associated with addressing it.

KEY WORDS: Concrete Signature, Distributed Fiber Optic Sensing, Distributed Strain Sensing, Bridge Structural Health Monitoring.

1 INTRODUCTION

Distributed fiber optic sensing (DFOS) has emerged as a pivotal technology in the realm of structural health monitoring (SHM) in recent years. The applications of DFOS can be broadly classified into three primary categories: distributed temperature sensing (DTS), distributed acoustic sensing (DAS), and distributed strain sensing (DSS). All these applications exploit backscatter effects arising from inhomogeneities within optical fibers. The principal types of backscatter effects include Raman, Brillouin, and Rayleigh backscattering [1, 2].

Within the scope of SHM of concrete structures, DSS has gained considerable attention, as it offers continuous strain measurements in structures, a significant advantage over traditional measurement systems such as strain gauges or inductive transducers [3]. DSS utilizing Rayleigh backscattering (optical frequency domain reflectometry) achieves a high spatial resolution of up to 0.65 mm with an accuracy of 1 µm/m [4], albeit with a sensing range constrained to approx. 100 m [5]. Therefore, its principal applications lie in the evaluation of failures, damages and local effects in concrete structures, particularly in the realms of crack detection and crack width calculation [6, 7].

Crack detection with DSS is predicated on peak identification, while the subsequent quantification of crack width relies on minima or midpoint approaches to ascertain the influence length of the crack to find out the borders for linear integration. Hence, it is important to distinguish clearly between peaks and minima attributable to cracks and those arising from other factors present in DSS readings [6, 7].

However, literature regarding DSS based on Rayleigh backscattering in concrete structures frequently reports local effects that do not correlate with disturbances originating from the measurement principle, such as noise or strain reading anomalies [8-11]. These local effects, subsequently referred to as the *concrete signature*, appear to evolve over time, maintaining a consistent position, thereby complicating the interpretation of DSS readings, particularly concerning crack detection and crack width evaluation, as well as for the identification of tension wire breakages [12].

Given that current publications on DSS employing Rayleigh backscattering predominantly rely on laboratory assessments or short-term field trials, this paper aims to investigate the phenomenon of evolving *concrete signature* in DSS readings over various time scales. To achieve this objective, DSS data from the openLAB research bridge in Bautzen, Germany, are analyzed [13, 14]. A picture of the openLAB research bridge is given in Figure 1.

The DSS dataset analyzed encompasses the production of precast elements, the installation phase, and the operational phase of the bridge, extending over a total sensor length of 1.5 km [13]. For the purposes of this analysis, a single beam will be selected to examine the development of the *concrete signature* along with the potential underlying factors and their implications. Ultimately, the study will elucidate the impact of *concrete signature* on DSS reading evaluation and its potential significance.

DOI: 10.3217/978-3-99161-057-1-099

Figure 1. OpenLAB research bridge in Bautzen, Germany (Stefan Göschel)

2 CONCRETE SIGNATURE

Although *concrete signature* is recognizable in the majority of publications [12, 15, 16], only a few commented it briefly [8-11, 17]. For instance, Richter et al. highlighted the emergence of local effects that are not associated with disturbances in the measurement system [9]. Becks et al. reported fluctuations of up to 200 µm/m in DSS readings from sensors adhered to the concrete surface, attributing these variations to local strain changes within inhomogeneous concrete [8]. Weisbrich et al. provided a similar explanation, conducting laboratory tests with concrete specimens that had Ormocer coated sensors glued to the surface, to reinforcement, and embedded in the concrete matrix [11]. They indicated that "inhomogeneities and imprecision of the concrete" could account for fluctuations in DSS readings observed during their tests [11]. Additionally, Sieńko et al. reported on micro-cracks resulting from thermal shrinkage during the concrete hardening process in laboratory tests, which correspond in size to the phenomena described by Becks et al. [8, 10]. Despite these effects being identified and illustrated in diagrams across numerous publications, there has yet to be a thorough investigation into their underlying causes and behaviors.

3 METHODOLOGY

To investigate the development and properties of *concrete signature* over various time scales, DSS readings from a fiber optic sensor placed in a 15 m prestressed bridge beam of the openLAB research bridge in Bautzen, Germany have been analyzed. The beam FT1.1 features a T-shaped cross-section and is prestressed. The beam is made from C20/25 standard concrete using granite and quartzite aggregates, with a maximum aggregate size of 16 mm.

The fiber optic sensor analyzed is an EpsilonSensor, 3 mm, ripped from Nerve-Sensors [18], where the fiber itself is embedded within a monolithic core out of polyester fibers and epoxide. It is situated at the bottom of the beam within the concrete matrix and is securely fixed to the stirrups using cable ties. The sensor was interrogated by an ODiSi6100 system from Luna Inc. [5], utilizing a gage pitch of 1.3 mm.

Figure 2 and Figure 3 are showing the placement of the sensor within beam FT1.1. Figure 2 illustrates the sensor placement within the beam FT1.1 at openLAB, while Figure 3 is a picture of the fiber optic sensor (red) within the reinforcement cage during the production of FT1.1.

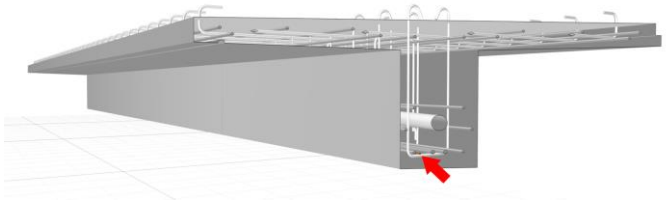

Figure 2. Sensor placement of the fiber optic sensor at beam FT1.1 in span 1 of the openLAB in Bautzen, Germany.

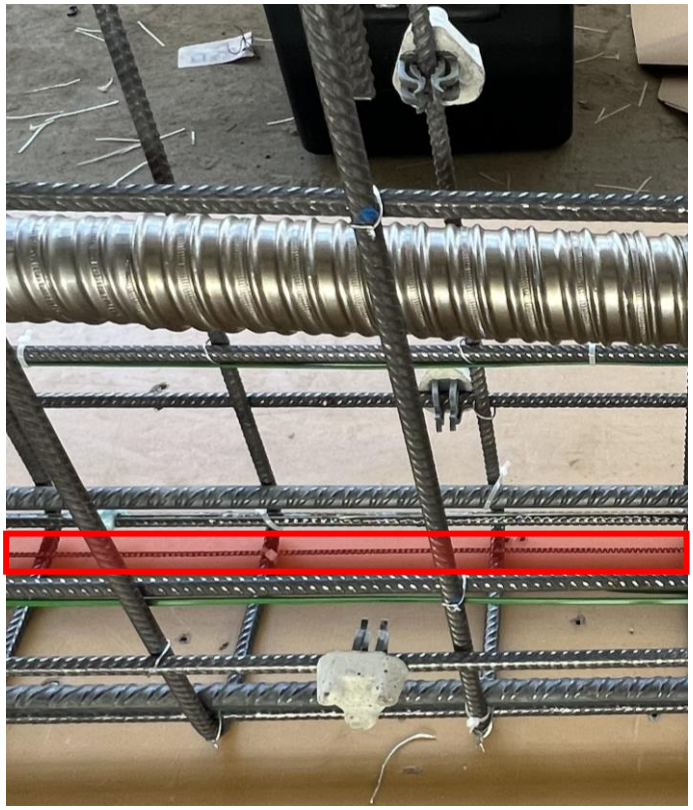

Figure 3. EpsilonSensor 3 mm ripped with the reinforcement cage of FT1.1 in span 1 of the openLAB in Bautzen, Germany.

In addition to DSS readings, temperature measurements with Gaia 200 of Maturix [19] using thermocouples type K inside the concrete took place during hydration. Later, during

DOI: 10.3217/978-3-99161-057-1-099

prestressing and operation, the concrete temperature was measured using Testo 176T4 [20] with thermocouples of type K at five points inside the beam. In the operational phase, a combi-sensor continuously measuring air temperature and air humidity was installed next to the beam.

The DSS readings have not been compensated for temperature variations, either regarding optical or material effects. Compensation for material effects entails addressing the thermal expansion of both the sensor materials and the host material. In the case of concrete as the host material, this is typically accomplished by utilizing the overall thermal expansion coefficient of concrete [16]. For optical effects, temperature compensation related to changes in refractive index is achieved by applying the temperature calibration constant of the fiber and calculating the spectral shift based on the temperature difference [21]. Given that only gradual temperature changes occur within concrete elements, neither effect significantly impacts the local, distinctive manifestation of the *concrete signature*.

The analysis involved varying the DSS readings tare to examine the redevelopment of the concrete signature across different time scales and for comparisons. Thereby, tare defines the point where the DSS reading was set to zero line again.

4 RESULTS

During the time scales under consideration, the global stress in the beam is changing several 100 µm/m due to temperature changes, load, creep, and shrinkage. However, the focus of this study is the development of the local *concrete signature*. Thus, a representative segment of 2 meters from the DSS readings, collected at specific timestamps, is presented to elucidate the data. The diagram areas delineate a section of 200 µm/m, visualized through a grid structured in increments of 50 µm/m. The orientation of the readings was selected based on the mean value located at the midpoint of the y-axis to effectively showcase the manifestation of the *concrete signature*.

The investigation initiates with the first 24 hours of the hydration phase of concrete, aiming to analyze the initial development of the *concrete signature*. For that the DSS readings have been referenced to the beginning of the hardening.

Figure 4 depicts the evolution of the *concrete signature* throughout hydration. The timestamp 0 hours signifies the beginning of the hardening process and the tare for the following DSS readings; consequently, the DSS reading establishes a baseline of zero. After 2 hours, initial fluctuations are observed, although the DSS readings remain relatively smooth. After 6 hours, a pronounced signature emerges, exhibiting an increasing trend until 12 hours, ultimately reaching a value range around the mean of approx. ±80 µm/m and a standard deviation of approx. 22.6 µm/m. Thereafter, the signature exhibits a decreasing trend until the concluding DSS reading at 24 hours with a value range of ±75 µm/m and a standard deviation of 20.4 µm/m. Notably, significant peaks are apparent between 2 hours and 6 hours, with DSS readings at 24 hours remaining considerably elevated.

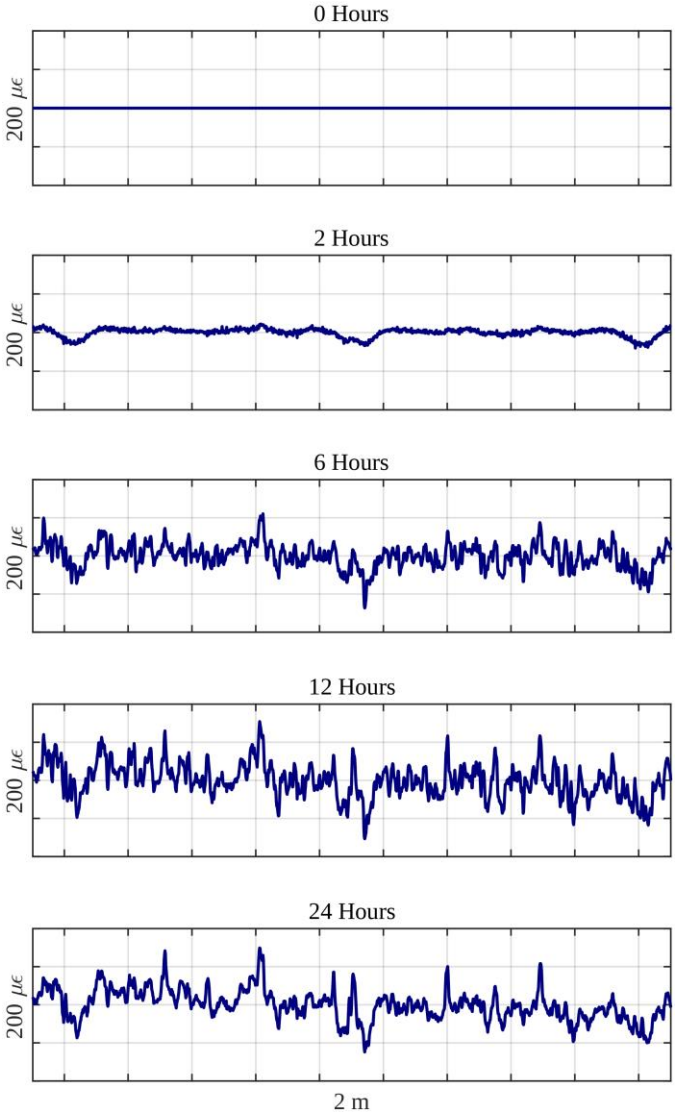

Figure 4. Distributed strain sensing readings during the first 24 hours of hydration.

During the hydration, a notable increase in the temperature of the concrete was observed, reaching a maximum temperature differential of 22.5 K relative to the tare readings at 0 hours. Figure 5 shows the temperature development during the hydration process as well as the temperature difference ΔT for the selected DSS readings to the tare reading at 0 hours.

DOI: 10.3217/978-3-99161-057-1-099

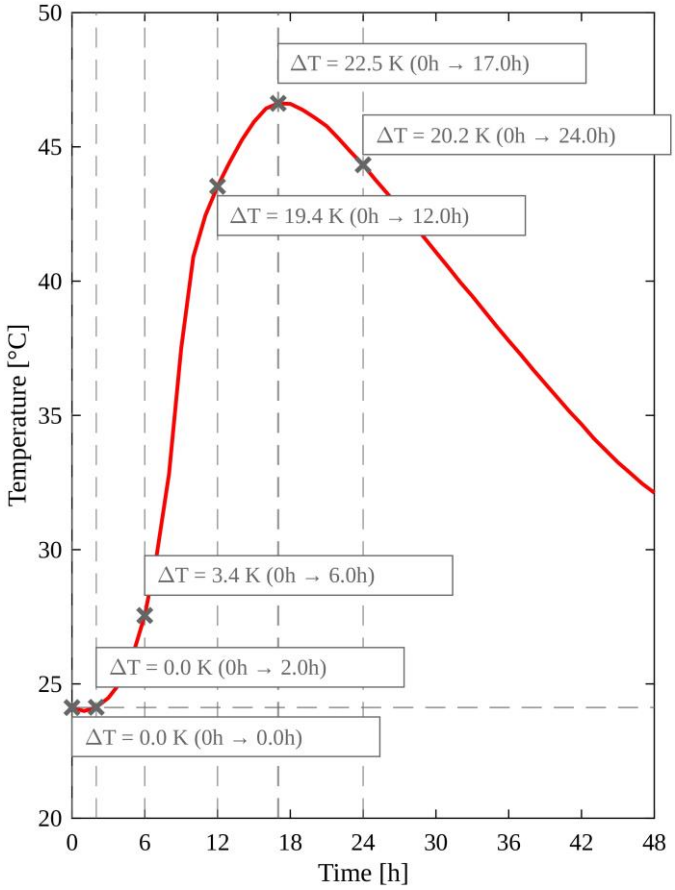

Figure 5. Temperature measurements during hydration.

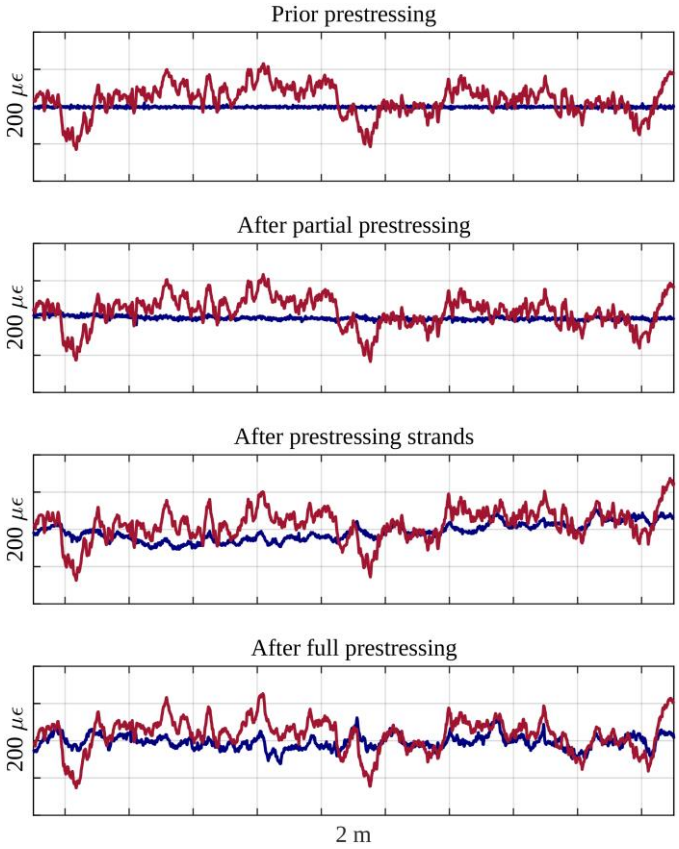

Figure 6. Distributed strain sensing readings during prestressing process (red: DSS readings with tare before hydration, blue: DSS readings with tare before partial prestress).

The prestressing process was subsequently analyzed with respect to the tare prior to hydration and the tare prior to prestressing. This included assessments prior prestressing the tendon, after partial prestressing the tendon in subsequent bonding 33 % and after prestressing strands in immediate bonding at a concrete age of 5 days. Followed by DSS readings after full prestressing of the tendon 100 % in subsequent bonding at concrete age of 15 days.

Figure 6 illustrates the evolution of the *concrete signature* throughout the prestressing process. The red lines represent the DSS readings with tare before hydration, while the blue lines indicate the DSS readings with tare before partial prestress, marked by the zero line at the timestamp just prior prestressing. Regardless of the tare used, the *concrete signature* in both DSS readings shows an increase and noticeable similarities.

A comparison of DSS readings across the different tares reveals that primary features consistently re-emerge during the prestressing process, also after taring prior to prestressing. Specifically, the *concrete signature* with tare before hydration reaches a maximum value range according to the mean of ±69 µm/m and a standard deviation of 22.1 µm/m, whereas the *concrete signature* with tare before prestressing reaches a maximum value range around the mean of ±31 µm/m and a standard deviation of 11.8 µm/m.

During the prestressing process, the concrete temperature changed less than 1 K. Compared to the tare before hydration the temperature changed approx. -4.9 K.

Finally, the *concrete signature* was assessed over one year with no traffic load during the DSS readings. The tare is established after finishing construction at the beginning of the operation phase (0 Months). Figure 7 illustrates the evolvement of the *concrete signature* during the operation. It is noteworthy that the *concrete signature* is already significantly redeveloped after three months. The increasing trend of the strain values from the left to the right side of the diagram in each DSS reading is due to the bending moment in the beam bearing on the columns. To quantify the *concrete signature* despite the bending effects, a sliding mean with a window of 380 (approximately 0.5 m at a gage pitch of 1.3 mm) was applied (Figure 7 dashed line). This approach yields a maximum value range of the concrete signature around the sliding mean of approximately ±29 µm/m at six months and a maximum standard deviation of 8.1 µm/m at 12 months.

After two months, distinct patterns of regular increases and decreases, occurring approx. every 15 cm, become apparent and are clearly noticeable after six months.

DOI: 10.3217/978-3-99161-057-1-099

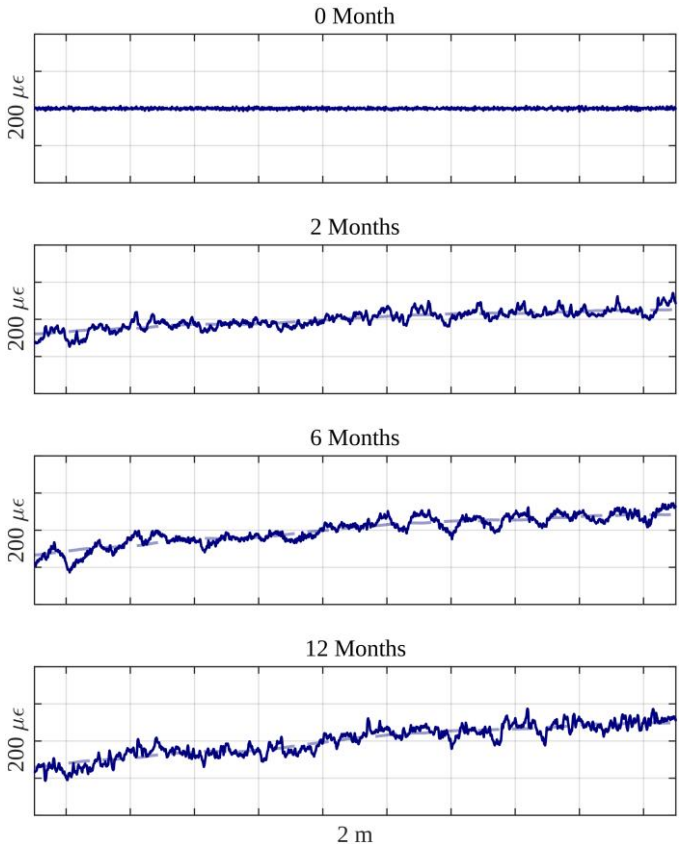

Figure 7. Distributed strain sensing readings during one year of operation.

During the operation, the beam was exposed to environmental conditions, resulting in permanent changes in air temperature and humidity. Concrete temperature, air temperature and air humidity changes regarding the tare measurement at 0 months are presented in Table 1.

Table 1. Temperatures and humidity changes during the selected DSS readings regarding to the tare at 0 months.

DSS reading	ΔT_c [K]	ΔT_a [K]	ΔrH_a [%]
0 months	0	0	0
2 months	+11.4	+17.0	+12.37
6 months	+10.5	+19.6	+6.81
12 months	-3.6	-1.54	+56.01

5 DISCUSSION

It has been demonstrated that the *concrete signature* begins to develop during the hydration process, with certain features remaining consistent over time. In the chosen DSS readings the most prominent signature occurs at 12 hours, which correlates with the highest temperature reached, leading to relation between the *concrete signature* and the temperature behavior of the concrete matrix. The temperature expansion coefficients of the various components of the concrete matrix—such as granite, quartzite, and cement stone—differ substantially (as shown in Table 2), thus the distinct expansions of these materials could be recorded by the sensor.

Table 2. Thermal expansion coefficients [22].

Component	Coefficient of thermal expansion αT [-]
Granite, Quarzporphyr	7.4 × 10−6
Basalt, Diorite, Gabbro	6.5 × 10−6
Quartz sand/gravel	11.0 × 10−6
Quarzite	11.8 × 10−6
Cement matrix (min)	10.0 × 10−6
Cement matrix (max)	23.0 × 10−6

A temperature increase of 19.4 K, like for the 12 hours DSS reading, induces a temperature strain of approx. 140 µm/m for granite, about 130 µm/m for basalt, and around 200 µm/m for liquid cement. This results in strain variations of up to 65 µm/m, close to the variation visible in the DSS reading at 12 hours. However, it is important to note that the thermal expansion coefficient of the cement matrix increases during hydration and decreases with diminishing humidity [22]. Additionally, throughout the hydration process, the modulus of elasticity, concrete strength, and, as a result, creep behavior exhibit continuous variations [23], which may also affect the signature.

The decrease of the signature at 24 hours might be due to the cooling as well as relaxation effects. The peaks observed after cooling can be attributed to the shrinkage of the cement matrix in relation to the aggregates. The more prominent peaks may be indicative of micro-cracks formed as a result of this shrinkage, as described by Sieńko et al. [10]. However, the regular spatial appearance of these peaks suggests the influence of structural elements such as stirrups or cable ties used for sensor fixation may also contribute.

During the prestressing process temperature remains almost constant. However, even after taring before prestressing, the *concrete signature* begins to redevelop. This suggests that the concrete signature is also influenced by load changes, leading to creeping effects. The creep behavior in concrete is affected by the Young's modulus, which varies based on age, aggregate size and shape, its deformation characteristics, and the ratio of cement paste or mortar to aggregates [23]. Considering the use of two aggregate types with differing shapes, sizes, and deformation characteristics, variations in their respective Young's moduli are expected. These differences can significantly influence their creep behavior, potentially affecting the DSS readings.

Similarly, the *concrete signature* continues to redevelop during the operational phase even after taring in the beginning. In this phase, all the potential influencing factors previously mentioned are at play. Environmental changes, such as fluctuations in temperature and humidity, contribute to swelling, shrinking, and thermal expansion. Additionally, there are creeping effects resulting from the prestressing and the dead weight of both the beam and the cast-in-place concrete slab.

The interaction of these effects, combined with the heterogeneous nature of the concrete matrix, leads to a continuous change in the *concrete signature*. Noteworthy is, that the maximum value range of concrete signature apparently increases with the concrete temperature. Additionally, the most significant fluctuations in the *concrete signature*, as indicated by the highest standard deviation, occur at an elevated relative air humidity level, which serves as an indicator of increased

DOI: 10.3217/978-3-99161-057-1-099

moisture in the concrete. However, due to the multitude of simultaneous effects, it is challenging to isolate and quantify the impact of each individual factor on the *concrete signature*.

The observed regular increases and decreases every 14 to 15 cm in certain sections may be attributed to the placement of stirrups, which are distributed approximately every 15 cm in the corresponding section of the beam. It is important to note that the concrete analyzed here is still relatively young (with the last DSS reading taken at an age of 19 months), which may result in greater fluctuations in the *concrete signature* due to more pronounced creeping effects in younger concrete.

Conceivable would also be that there are also effects from the reaction of the sensor coating itself. Fluctuations in the concrete moisture and concrete temperature can lead to expansion effects in the material, which can be transferred to the fiber. This effect is for example used for polyimide-coated fibers in order to measure humidity [24]. However, for coating out of polyester fibers and epoxide these effects can be neglected, since epoxide (epoxy glue) is used to insulate fibers from the surrounding moisture [24].

Regardless of the specific time episode being analyzed, the manifestation of the *concrete signature* is always dependent on the selected tare. While the tare does alter the resulting *concrete signature* itself - such as the position of the peaks - it does influence the prominence (e.g, the height of the peaks), as illustrated in the prestressing process. This distinction is crucial during data evaluation, as an appropriately chosen tare can enhance the *concrete signature* for analysis or diminish it to isolate other factors under scrutiny, such as tension wire breakages. However, the ability to reduce the *concrete signature* in this manner is contingent upon DSS readings taken in temporal proximity to the effect being analyzed, given that the *concrete signature*, at least in the evaluated DSS readings, tends to redevelop rapidly.

6 CONCLUDING REMARKS

It has been shown that *concrete signature* develops over various time episodes, ranging from several hours to several months. Potential environmental factors influencing this phenomenon include temperature, humidity, and load, which can lead to thermal expansion, shrinkage, swelling, and creep, as well as localized disturbances from structural elements like cable ties or reinforcement. Additionally, it is crucial to consider factors intrinsic to the concrete matrix, particularly the differing responses of aggregates and the cementitious matrix to these environmental influences. The age of the concrete itself may also play a significant role, since creeping and shrinkage depend on concrete maturity.

In this study, *concrete signature* achieved a maximum value range of ±75 µm/m, which considerably affects crack detection and width calculation, as peak detection and minima approaches may not work accurately. Moreover, identifying micro-cracks or instances of tension wire breakage may prove challenging, as these phenomena produce effects smaller than those associated with *concrete signature*. Consequently, the priority will be to develop effective compensation methods to ensure the reliability of data from digital signature systems (DSS).

However, gaining insights into the causes and influences on *concrete signature* could provide a better understanding of concrete behavior related to load, creep, shrinkage, and thermal expansion. This understanding would facilitate more accurate assessments of structural behavior, for instance, by refining calculations pertaining to creep effects as outlined in EC2. Moreover, *concrete signature* may present opportunities for quality assessment during production through the examination of material inhomogeneities like gravel nests.

To gain a deeper understanding of the causes and factors influencing *concrete signature* in DSS readings, systematic testing is currently underway. Initial experiments are designed to isolate these impact factors and observe the resulting responses of the concrete matrix at the meso-level. Building on this knowledge, compensation methods and knowledge extraction techniques can subsequently be developed and evaluated in field tests.

ACKNOWLEDGMENTS

This paper outlines findings from the research projects FOSsure (Fiber optic sensors for reliable condition assessment of solid bridges) and IDA-KI (Automated evaluation of monitoring data from infrastructure structures) funded by the Federal Ministry for Digital and Transport, Germany, within the innovation program mFUND (funding references: 19FS2075B and 19FS2013C).

Additionally, it outlines findings from the Return (Multi-risk science for resilient communities under a changing climate) This Foundation, with headquarters in Corso Umberto I, 40 80138 Napoli (NA), is founded by National Resilience and Recovery Plan (NRRP).

REFERENCES

[1] Berrocal, C. G., I. Fernandez, and R. Rempling. 2020. “Crack monitoring in reinforced concrete beams by distributed optical fiber sensors” Struct. Infrastruct. E., 17(1):124–139, doi:10.1080/15732479.2020.1731558.

[2] Howiacki, T., R. Siénko, Bednarski, and K. Zuziak. 2023. “Crack Shape Coefficient: Comparison between Different DFOS Tools Embedded for Crack Monitoring in Concrete” Sensors, 23(2):566, ISSN 1424-8220, doi:10.3390/s23020566.

[3] Monsberger, C. and W. Lienhart. 2021. “Distributed Fiber Optic Shape Sensing of Concrete Structures” Sensors, 21:6098, doi:10.3390/s21186098.

[4] Janiak, T., H. Becks, B. Camps, M. Classen, and J. Hegger. 2023. “Evaluation of distributed fiber optic sensors in structural concrete”. Materials and Structures, 56(9), 159, doi:10.1617/s11527-023-02222-9.

[5] Luna Innovations Incorporated. 2021. “User’s Guide ODiSI 6” Tech. rep., Luna Innovations Incorporated.

[6] Herbers, M., B. Richter, and S. Marx. 2024. “Rayleigh-based crack monitoring with distributed fiber optic sensors: experimental study on the interaction of spatial resolution and sensor type” Journal of Civil Structural Health Monitoring:1–25, doi:10.1007/s13349-024-00896-5.

[7] Richter, B., M. Herbers, and S. Marx. 2023. “Crack monitoring on concrete structures with distributed fiber optic sensors—Toward automated data evaluation and assessment” Structural Concrete, 25:1465–, doi:10.1002/suco.202300100.

[8] Becks, H., A. Baktheer, S. Marx, M. Classen, J. Hegger, and R. Chudoba. 2022. “Monitoring concept for the propagation of compressive fatigue in externally prestressed concrete beams using digital image correlation and fiber optic sensors” Fatigue Fracture of Engineering Materials Structures, 46, doi:10.1111/ffe.13881.

[9] Richter, B., L. Ulbrich, M. Herbers, and S. Marx. 2024. “Advances in data pre-processing methods for distributed fiber optic strain sensing” Sensors, 24(23):7454.

[10] Siénko, R., Ł. Bednarski, and T. Howiacki. 2021. “Distributed Optical Fibre Sensors for Strain and Temperature Monitoring of Early-Age Concrete: Laboratory and In-situ Examples” in F. Kanavaris, F. Benboudjema, and M. Azenha, eds., International RILEM Conference on Early-Age and Long-Term Cracking in RC Structures, Springer International Publishing, Cham, ISBN 978-3-030-72921-9, pp. 77–87.

DOI: 10.3217/978-3-99161-057-1-099

[11] Weisbrich, M., D. Messerer, and K. Holschemacher. 2023. “The Challenges and Advantages of Distributed Fiber Optic Strain Monitoring in and on the Cementitious Matrix of Concrete Beams” Sensors, 23(23), ISSN 1424-8220, doi: 10.3390/s23239477.
[12] Richter, B., E. Will, M. Herbers, and S. Marx. 2025. “Detection of prestressing wire breaks in post-tensioned concrete structures using distributed fiber optic strain sensing” [submitted].
[13] Herbers, M., B. Richter, J.-H. Bartels, T. Al-Zuriqat, K. Smarsly, and S. Marx. 2024. “openLAB - A large-scale demonstrator for advancing digital twin developments of bridges”.
[14] Technichal University of Dresden. “openLAB”. Accessed June 2025. https://tu-dresden.de/bu/bauingenieurwesen/imb/forschung/grossprojekte/openLAB?set_language=en
[15] Boros, V., A. Vorwagner, D. Prammer, and W. Lienhart. 2024. “Application of Embedded Distributed Fiber Optic Sensors on a Highway Bridge as a Support for Bridge Inspections”.
[16] Alj, I., M. Quiertant, A. Khadour, Q. Grando, and K. Benzarti. 2022. “Application of Distributed Optical Fiber Sensing Technology to the Detection and Monitoring of Internal Swelling Pathologies in Massive Concrete Blocks” Sensors, 22(20), ISSN 1424-8220, doi: 10.3390/s22207797.
[17] Zdanowicz, K., T. Howiacki, R. Siénko, and S. Marx. 2021. “DFOS measurements of strain development in textile reinforced concrete slabs with expansive admixture during setting and hardening”.
[18] Nerve-Sensors. “EpsilonSensor”. Accessed June 2025. https://nerve-sensors.com/wp-content/uploads/2024/10/EpsilonSensor_DE.pdf.
[19] Maturix. “Gaia 200”. Accessed June 2025. https://maturix.com/sensors/gaia-200/
[20] Testo Saveris GmbH. Accessed June 2025. https://static.testo.com/image/upload/HQ/testo-176-t3-t4-datenblatt.pdf
[21] Luna Innovations Incorporated. 2014. „Distributed Fiber Optic Sensing: Temperature Compensation of Strain Measurement“. https://lunainc.com/sites/default/files/assets/files/resource-library/LT_TD_EN-FY1402_TempComp1.pdf
[22] Spilker, A. 2024. Zur experimentellen Bestimmung der Wärmedehnzahl von Beton im Straßenbau, Ph.D. thesis, Institut für Werkstoffe im Bauwesen der Universität Stuttgart.
[23] Meyer, L. 2007. Zum Einfluss der Kontaktzone bei der Modellierung des Elastizitätsmodulus von Beton, Ph D. thesis, Rheinisch-Westfälische Technische Hochschule Aachen.
[24] Wang, L., N. Fang, and Z. Huang. 2012. „Polyimide-coated fiber Bragg grating sensors for humidity measurements“. InTech.